Investigation of the Stochastic Oregonator by the Probability Cellular Automaton: Frequency-Multiplying Bifurcation

Vladimir K. Vanag

Center of Photochemistry, Russian Academy of Sciences, 117421, Novatorov Str., 7A, Moscow, Russia

Received: February 13, 1997; In Final Form: May 6, 1997[⊗]

The method of probability cellular automaton (PCA) has been used to simulate turbulent stirring, molecular diffusion, and the reactions of the stochastic Oregonator in each cell of the automaton and to model the bifurcation of oscillation frequency multiplication discovered earlier in the Belousov−Zhabotinsky reaction in water-in-oil Aerosol OT microemulsion. At large constants of mass exchange between the adjacent PCA cells (k_{ex}), the system demonstrates oscillations whose shape and period (T_∞) are fully identical with those obtained from the solution of the ordinary differential equations. When k_{ex} decreases, the period T shortens and reaches the limit T_m at $k_{ex} \leq k_{cr}$. The smaller the volume V_c assigned to a PCA cell and the slower the system's approach to the critical concentration of the inhibitor $[Br^-]_{cr}$, the higher the ratio T_∞/T_m. The stochastisity of microoscillators is the source of new frequencies.

1. Introduction

The investigation of the Belousov−Zhabotinsky (BZ) reaction[1] occurring in water nanodroplets of the water-in-oil AOT microemulsion in organic media (AOT = sodium 1,4-bis(2-ethylhexyl)sulfosuccinate)[2] opens new possibilities for studying the effect of concentration fluctuations on nonlinear chemical reactions because the amplitude of fluctuations in micro- and nanovolumes (represented here by water nanodroplets of the AOT microemulsion) becomes considerably larger. From the physical point of view, water-in-oil AOT microemulsion is a multitude of water nanodroplets surrounded by a monolayer of AOT molecules whose long hydrophobic tails are directed to an organic solvent while the polar headgroups are directed toward the water core of a micelle.[3] The size of a micelle (a micelle is a water core + a wall made of surfactant molecules) is independent of the concentration of a micelle in the microemulsion and is determined by the ratio (ω) of the molar concentrations of water and AOT.[4]

$$\omega = [H_2O]/[AOT] \tag{1}$$

The radius of the micellar water core (R_w) is estimated approximately as[5,6]

$$R_w \text{ (in nm)} \cong 0.175\omega \tag{2}$$

The concentration of micelles (C_m) is proportional to the volume fraction of the aqueous pseudophase (ϕ_w)

$$C_m = \phi_w/(V_m N_A) \tag{3}$$

where V_m is the volume of the micellar water core, $V_m = 4\pi R_w^3/3$, N_A is the Avogadro number, and

$$\phi_w = V_w/(V_{oil} + V_w) \tag{4}$$

where V_w is the volume of the aqueous phase which should be added to the volume V_{oil} of the AOT solution in organic solvent to prepare the AOT microemulsion.

When C_m exceeds some critical concentration, the micelles start forming clusters, which at rather high ϕ_w become percolation.[7,8] This is confirmed by the electrooptic Kerr-effect and electric conductivity measurements (the conductivity, for example, displays percolation transition, changing over many orders of magnitude). Despite a relatively large size of percolation clusters, the microemulsion remains optically transparent until the value ϕ_w reaches the cloud point ($\phi_w \cong 0.5-1$), beyond which phase separation into two phases occurs. Regrettably, the detailed structure and dynamics of AOT microemulsion loaded with concentrated sulfuric (or other) acid (0.1−0.6 M) where the BZ reaction runs is not known. Therefore we shall base this study on the structure and dynamics of an AOT microemulsion where the water nanodroplets are loaded with low concentrations (<0.01 M) of some substances at neutral pH.

According to these considerations, mass exchange between water nanodroplets of a dilute microemulsion occurs as a result of fusion−fission of the micelles.[5] On average, each 100th or 1000th collision of the micelles leads to fusion, and the bimolecular constant of the mass exchange rate is estimated as 1×10^7 M^{-1} s^{-1}.[4,5] It is suggested that as a result of the fusion of two micellar water cores their content is mixed completely, after which the micelles are separated. In micellar clusters, the micelles keep their closed structure,[9] and the constant of a particle jump (walk frequency) between micelles of the same cluster (intracluster displacement) is estimated as $(2-4) \times 10^5$ s^{-1}.[10] Mass exchange between clusters is a very slow process, by 2−3 orders slower than the rate of mass exchange between separate micelles. All reagents and most intermediates of the BZ reaction are water soluble. Thus, the AOT-BZ reaction may be considered to run mostly in water nanodroplets of AOT microemulsion.

While studying the ferroin-catalyzed AOT-BZ reaction, we discovered some new effects. Among them were the dependence of oscillation area in phase space on the size and concentration of water nanodroplets,[11] extraordinary high photosensitivity of the AOT-BZ reaction,[12] the square dependence of the rate of autocatalytic growth in $[HBrO_2]$ and the oxidized form of the catalyst, [ferriin], on $[NaBrO_3]$,[13] and a new bifurcation[14] called by us the frequency-multiplying bifurcation. This bifurcation, displayed as a spontaneous multiplication of oscillation frequency by 2, 2.5, 3, or 4 and as a simultaneous sharp decrease in oscillation amplitude, occurs only in micro-

[⊗] Abstract published in *Advance ACS Abstracts,* August 15, 1997.

S1089-5639(97)00561-6 CCC: $14.00

TABLE 1: Dependence of L (Size Range of the Randomly Chosen Squares) and N_L (Number of Times the Squares of a Given Size Range Were Sampled) at a Single Time Step on the Stirring Level, *Lev*, at $N_0 = 64^2$, $N_0 = 32^2$, and 16^2

Lev				N_L		
$N_0 = 16 \times 16$	$N_0 = 32 \times 32$	$N_0 = 64 \times 64$	L	$N_0 = 16 \times 16$	$N_0 = 32 \times 32$	$N_0 = 64 \times 64$
		1	64−56			1
	1	2	32−26		1	4
1	2	3	16−10	1	4	16
2	3	4	8−4	8	32	128
3	4	5	4−2	64	256	1024

emulsions with a high volume fraction of the aqueous pseudophase ϕ_w (when $\phi_w \geq 0.05$). At such values of ϕ_w in the AOT microemulsion, the percolation clusters are formed,[7,15] and the viscosity of microemulsion sharply increases, reaching 10 cP and more.[16] We suggested[14] that the clusters formed in microemulsion and loaded with the reagents of the BZ reaction may be regarded as the stochastic microoscillators (MO), i.e., the oscillators whose dynamics are considerably affected by the smallness of the amount of particles in microvolume (MV), this fact being expressed both in the enhancement of inner fluctuations and in the probability character of chemical reactions running in MVs. We also suggested that the frequency-multiplying bifurcation is connected with the specific interaction in the assembly of diffusionally coupled stochastic MOs.

A great number of articles is devoted to the study of coupled oscillators (see, for instance, the review by Epstein and Showalter[17]). Fewer studies deal with the interactions of chaotic or stochastic oscillators. These studies are mostly restricted to the consideration of two coupled oscillators.[18] We are unaware of any works devoted to the interaction of many stochastic MOs, especially under the conditions of their turbulent stirring.

The aim of the present work is a theoretical study of the oscillatory AOT-BZ reaction which we represented as a sum of many diffusionally coupled stochastic MOs under their turbulent stirring. As a model of the BZ reaction, the Oregonator model[19] was chosen being the simplest one. Thus we shall consider the assembly of stochastic Oregonators.

This system relates to most complex systems of the "reaction−diffusion−convection" type + fluctuations. To solve such systems we developed the method of the probability cellular automaton (PCA).[20] With the PCA method, in which the Monte Carlo procedure was applied, we were able to explain the stirring effect discovered earlier in the closed BZ reaction[21] and to prove that the average velocity of the motion of the turbulently stirred media affects the behavior of nonlinear chemical reactions proceeding in the media. This effect emerges at the level of the interaction between hydrodynamic fluctuations in the velocities of liquid elements (microeddies) and large-scale concentration fluctuations in key intermediates of the reaction because the spatial characteristic lengths of these fluctuations nearly coincide for such liquids as water. In this work we used the PCA method to study how the coupling strength (mass exchange coefficient) between MVs and the spatial size of MVs affect the oscillation frequency of the whole oscillator−Oregonator assembly as a unified system under turbulent stirring.

2. PCA Method for the Oregonator Model

A detailed description of the PCA method for the stochastic Oregonator can be found elsewhere.[20] Here we shall only briefly outline the principles of the PCA functioning and some innovations made. The PCA independently models three processes: (a) molecular diffusion, (b) turbulent stirring, and (c) chemical reactions. In this work all the processes are mostly modeled on the lattice consisting of $N_0 = N^2$ (N is an integer) $= 32^2$ or $N_0 = 64^2$ equal elementary cells. An elementary cell is assigned to have a volume V_c and linear size $l_c = (V_c)^{1/3}$. The value V_c is used to determine the probability of bimolecular reactions being simulated independently in each elementary cell. The lattice is self-closed, i.e., the opposite sides of the lattice are assumed to be adjacent.

Block "Diffusion". Molecular diffusion is given by the probability $W(m,k|r,s)$ to find m and k particles at the moment $t + StepDif$ in two randomly chosen neighboring cells (in our case, the "central" cell has eight neighboring cells; coordination number = 8), if at the moment t they contained r and s particles of this sort, where *StepDif* is the constant time step which separates successive operations of diffusion modeling (procedure or block "diffusion"), then

$$W(m,k|r,s) = (r + s)!/(k!m!)\,(1/2)^k(1 - 1/2)^m \qquad (5)$$

The intensity of mass exchange (or, which is the same, of the molecular diffusion) is regulated either by the value *StepDif* or by the value $(ND)(N_0)$ of randomly chosen pairs of adjacent cells at one time step *StepDif*. The value of *ND* did not exceed 0.5. The ratio *ND*/*StepDif* determines the constant (or frequency) k_{ex} of particle jump into an adjacent cell.[20]

$$k_{ex} = ND/StepDif \qquad (6)$$

The value k_{ex} relates to the diffusion coefficient D_0:[20]

$$D_0 \cong k_{ex}\, l_c^2 \qquad (7)$$

The Oregonator model uses three independent variables X, Y, and Z: X = $HBrO_2$ is an activator, Y = Br^- is an inhibitor, and Z is a catalyst represented either cerium(IV) ion or ferriin ($Fe(phen)_3^{3+}$, phen = phenanthroline). Each of these particles has its own diffusion coefficient. In the PCA this is accounted for by using three various numbers of *ND* (ND_X, ND_Y, and ND_Z) and by independent application of the "diffusion" procedure for each variable at each time step *StepDif*.

Block "Stirring". Turbulent stirring (block "stirring") is performed in regular intervals of time (*StepMix*) by selecting a square $L \times L$ in size ($L < N$) in an arbitrary place of the lattice N_L times and by randomly pairwise rearranging the square's four quadrants. The stirring intensity is given by the time step *StepMix* and a number *Lev*. The larger the *Lev* and the smaller the *StepMix*, the higher the stirring intensity. For each *Lev* number there are the corresponding numbers N_L and L presented in Table 1. For instance, for the lattice 32×32 in size and *Lev* = 3 and with each time step *StepMix*, a square of the size $L \times L$, where L randomly assumes any of the values of 32, 30, 28, or 26, is chosen one time, the squares of the size from 16×16 to 10×10 are chosen four times, and the squares of the size from 8×8 to 4×4 are chosen 32 times. A detailed description of the "stirring" procedure is given elsewhere.[20]

The intensity of macromixing is characterized by the mixing rate constant k_{mix} determined in the experiments by mixing two equal parts of the lattice, whose cells are in different states n at the initial moment of time, where n is the number of particles

of the same sort; for example, $n = 0$ for the cells of one half and $n = 200$ for the cells of the other half of the lattice. The mixing rate constant k_{mix} was determined by fitting the experimentally obtained dependence of $(\sigma^2 - \sigma_{eq}^2)$ on time with the expression

$$(\sigma_0^2 - \sigma_{eq}^2) \exp(-k_{mix}t) \tag{8}$$

where σ^2 is the dispersion determined by the formula:

$$\sigma^2 = \frac{1}{N_0}\sum_{n=0}^{n_{max}}(n - \langle n\rangle)^2 N(n) \tag{9}$$

$$\langle n\rangle = \frac{1}{N_0}\sum_{n=0}^{n_{max}} n\, N(n) \tag{10}$$

$N(n)$ is the number of cells containing n particles of a given sort, σ_0^2 is the dispersion at the initial moment of time $t = 0$, σ_{eq}^2 is the equilibrium value of the dispersion at $t \to \infty$, and $\sigma_{eq}^2 = \langle n\rangle$. The constants k_{mix} are determined by the linear regression method[22] with *R*-squared values not less than 0.95−0.98. Such high *R*-squared values are explained by the fact that the dependencies of $(\sigma^2 - \sigma_{eq}^2)$ on t are practically the straight lines in the coordinates t, $\ln(\sigma^2 - \sigma_{eq}^2)$. Typical dependencies of $(\sigma^2 - \sigma_{eq}^2)$ on t at various k_{ex} are presented in the Supporting Information in Figure 1S.

The value k_{mix} depends on the rate of micromixing (diffusion) determined by the value k_{ex} and on the stirring rate determined by the values *StepMix* and *Lev*. When the rate of cell rearrangement is high enough, the constant k_{mix} is completely determined by the diffusion, so that $k_{mix} \cong k_{ex}$. The dependencies of k_{mix} on k_{ex} for various stirring levels *Lev* are presented in Figure 1A. The "stirring" procedure may become the limiting step of macromixing at smaller *StepMix* and *Lev*. The dependencies of k_{mix} on *StepMix* at various k_{ex} and *Lev* are shown in Figure 1B. It can be seen from Figure 1B that as *StepMix* decreases, the value k_{mix} tends to the limit that equals k_{ex} for the corresponding curve.

This model of the cells−MOs coupling somehow resembles the model of global coupling when each oscillator is coupled with all the rest. When the rate of macrorearrangement of the cells is great in comparison with k_{ex}, the probabilities averaged over some long time interval T (for example, over the oscillation period) that mass exchange between a randomly chosen cell and any other of the N_0 cells occurs are equal. The difference between this model and the global coupling is in the fact that, for this model, at a given moment of time t the mass exchange is possible only with the adjacent cells, which represents the facts.

Block "Chemistry". Five chemical reactions of the Oregonator model running independently in each elementary cell were simulated by the Monte Carlo method. At each time step τ (τ differs from *StepDif* and *StepMix*) for every cell, a random number θ ($\theta \in [0,1]$) was generated. If the relation $\theta < W_i$ held, the i-th reaction was realized, where W_i is the probability that a number of particles of the corresponding sort contained in an elementary cell (n) changes by the stoichiometric coefficient of the i-th reaction in the cause of the reaction being realized.

Table 2 presents the reactions of the Oregonator model, their first-order constants γ_i which control the reactions in nano- and microvolumes,[20,23] and the corresponding reaction rates and their probabilities W_i. Since the discrete variables n_X, n_Y, and n_Z, where n_X, n_Y, and n_Z are the numbers of particles X, Y, and Z, respectively, contained in an elementary cell with the volume V_c, may change only by the whole number, then the coefficient g is taken to be $g = 0.5$, and reaction R5 is interpreted as follows:

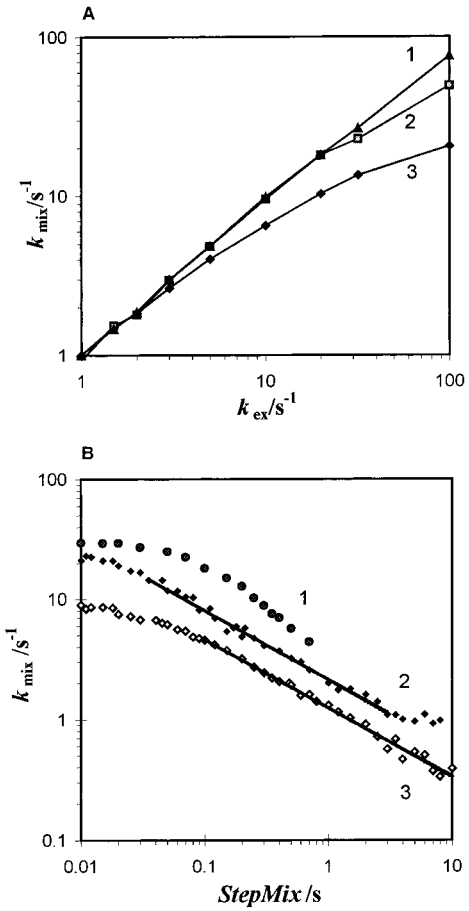

Figure 1. The dependence of the macromixing constant k_{mix} at various stirring levels *Lev* for the lattice of size $N_0 = 32^2$ on (A) the constant of mass exchange k_{ex} between the neighboring cells and (B) on the time step *StepMix* at various constants k_{ex}. PCA parameters: (A) *StepMix* = 0.05 s, *Lev* = 4 for curve 1, *Lev* = 3 for curve 2, *Lev* = 2 for curve 3; (B) for curve 1 *Lev* = 3 and $k_{ex} = 32\ s^{-1}$, for curve 2 *Lev* = 2 and $k_{ex} = 32\ s^{-1}$, for curve 3 *Lev* = 2 and $k_{ex} = 10\ s^{-1}$.

$$\begin{aligned} n_Z &\to n_Z - 2 \\ n_Y &\to n_Y + 1 \end{aligned} \tag{R5′}$$

with the probability of its run being $W_5/2$.

Time step τ was determined for each discrete moment of time from the relation

$$\tau = 0.1/\max\{q_i\} \tag{11}$$

where q_i are the rates of the i-th reactions presented in Table 2, while the values of n_X, n_Y, and n_Z are taken from the preceding moment of time. The step τ depends on the oscillation phase and varies, as a rule, from 10^{-5} to 10^{-2} s. As the number of particles in the cell increases in the cause of the reaction, the step τ decreases, and vice versa. The main characteristic parameters and constants of all three processes modeled by the PCA are summarized in Table 3.

3. The Values of Model Parameters

Our system's behavior is affected by many parameters. These are the reaction rate constants of the Oregonator model, mass

TABLE 2: Reactions of the Oregonator Model, Monomolecular Reaction Rate Constants (γ_i), Monomolecular Reaction Rates (q_i), and Corresponding Probabilities (W_i)[a]

no.	reactions	γ_i, s^{-1}	q_i, s^{-1}	W_i
R1	$A + Y \rightarrow X$	$k_1[A] = 0.02-0.06$	$k_1[A]n_Y$	$k_1[A]n_Y\tau$
R2	$X + Y \rightarrow 0$	$k_2/(V_cN_A)$	$(k_2/(V_cN_A))n_Xn_Y$	$(k_2/(V_cN_A))\ n_Xn_Y\tau$
R3	$A + X \rightarrow 2X + 2Z$	$k_3[A] = 2-6$	$k_3{}^n x = k_3[A]n_x$	$k_3[A]n_X\tau$
R4	$X + X \rightarrow 0$	$k_4/(V_cN_A)$	$(2k_4/(V_cN_A))n_X(n_X - 1)$	$(2k_4/(V_cN_A))n_X(n_X - 1)\tau$
R5	$Z + B \rightarrow gY$	$k_5[B] = 1$	$k_5[B]n_Z$	$k_5[B]n_Z\tau$

[a] $A = BrO_3^-$, B = malonic acid, $X = HBrO_2$, $Y = Br^-$, Z = catalyst in oxidized state, g is the stoichiometric factor, $g = 0.5$, V_c is the volume assigned to the PCA elementary cell, N_A is the Avogadro number, τ is the time step assigned to a single cycle of the program. Basic set of the constants k_i: $k_1 = 0.2\ M^{-1}\ s^{-1}$, $k_2 = 2 \times 10^5\ M^{-1}\ s^{-1}$, $k_3 = 20\ M^{-1}\ s^{-1}$, $k_4 = 2 \times 10^3\ M^{-1}\ s^{-1}$, $k_5 = 1\ M^{-1}\ s^{-1}$. $[B] \equiv b = 1$ M; $[A] = 0.3$ M or $[A] = 0.1$ M.

TABLE 3: Summary Table with the Main Parameters and Characteristics of All Three Processes Modeled by the PCA[a]

parameters	molecular diffusion	turbulent stirring	chemical reactions
time step through which a corresponding operation block is fulfilled	*StepDif*	*StepMix*	τ
number of operations in a block	$ND \times N_0$	$\sum_{1}^{Lev} N_L$	qN_0
probability of a single operation	$W(m,k\|r,s)$	W_s	W_i
pseudo-first-order constants of the process rate	k_{ex}	k_{mix}	γ_i

[a] Parameters *Lev*, N_L, and L are given in Table 1. Probabilities W_i and constants γ_i are given in Table 2. N_0 is the number of elementary cells in square PCA's lattice. q is the number of chemical reactions modeled; $q = 5$ for the Oregonator. i is the reaction number: $i = 1, ..., q$. The probability $W(m,k|r,s)$ and time step τ are determined by formulas 5 and 11, respectively. W_s is the probability that at least two out of four quadrants of a randomly chosen $L \times L$ square will be randomly pairwise rearranged during a single operation, $W_s = 3/4$. The parameters *StepDif*, *StepMix*, *ND*, N_0, *Lev*, $\gamma_i = f(k_i,V_c)$, V_c, and k_i were varied in the PCA model, but all of them remained constant through one computer experiment. The parameters k_{ex}, k_{mix}, and γ_i determine the main kinetic characteristics of the processes. k_{ex} is given by formula 6.

exchange constants k_{ex} (or diffusion constants D_0) for each variable of the Oregonator model, and the characteristics of macromixing *StepMix* and *Lev* integrated together with k_{ex} in the constant k_{mix}. Since our model is based on the AOT-BZ reaction, we turned to the real system to estimate all the possible values of these parameters.

The diffusion coefficients undertake considerable changes in comparison with the homogeneous aqueous media. In AOT microemulsion, the diffusion of the water-soluble particles localized in micelle water cores occurs as a result of fusion−fission of water nanodroplets diffusing in the organic phase. The characteristic constant k_{ex} of mass exchange between micelles is determined by the expression

$$k_{ex} = p_f k_d C_m \tag{12}$$

where k_d is the constant of the diffusion-controlled reactions, C_m is the concentration of micelles in the whole volume of microemulsion, p_f is the coefficient determining which part of the collisions between micelles leads to mass exchange. For the characteristic values of p_f, k_d, and C_m ($p_f = 0.001 - 1$, $k_d \cong 10^9 - 10^{10}\ M^{-1}\ s^{-1}$, and $C_m = 10^{-5} - 10^{-2}$ M), k_{ex} is equal to $10^2-10^8\ s^{-1}$. With the formation of large clusters, the constant k_d decreases by 1−2 orders of magnitude due to an increase in microemulsion viscosity and the value C_m is replaced by the concentration of clusters C_c and, accordingly, decreases by 1 − 3 orders of magnitude, while p_f becomes rather indeterminate because of the uncertainty in cluster structure and in the mechanism of mass exchange between clusters but is certain not to grow, $p_fk_d < 10^5\ M^{-1}\ s^{-1}$.[15,24,25] Hence, with cluster formation, the constant k_{ex} may decrease by 1−5 orders of magnitude, and $k_{ex} = p_fk_dC_c = 10^{-2}-10^3\ s^{-1}$. Therefore, the value k_{ex} should vary within the broad limits in our computer experiment.

Since k_{ex} is connected with D_0 by relation 7, where l_c may be regarded as the average distance between micelles (or between clusters in the case of their presence), $l_c \cong (C_mN_A)^{-1/3}$, and then D_0 may be estimated from eqs 3, 7, and 12 as

$$D_0 = p_fk_dC_m(C_mN_A)^{-2/3} = p_fk_d\,(3\phi_w/4\pi)^{1/3}/(R_wN_A) \tag{13}$$

For the characteristic values of p_fk_d, R_w, and ϕ_w ($p_fk_d = 10^7-10^8\ M^{-1}\ s^{-1}$, $R_w = 2-5$ nm, and $\phi_w = 0.1$), the D_0 is found to be $(1 \times 10^{-8}-2 \times 10^{-7})\ cm^2/s$.

For the AOT-BZ reaction catalyzed by ferroin, the following obstacle may prove to be significant. It is known[26] that the exchange of phenanthroline metallocomplexes between AOT micelles occurs at each collision of the micelles, i.e., $p_f \cong 1$ for ferroin. This is explained by phenanthroline solubility in long fatty ends of AOT molecules. The exchange of small water-soluble molecules and ions, like $HBrO_2$ and Br^-, occurs at each 100th collision of micelles, i.e., $p_f \cong 0.01$ for $HBrO_2$ and Br^-. Let us denote the constants k_{ex} and D_0 for particles X, Y, and Z as k_X, k_Y, k_Z and D_X, D_Y, D_Z, respectively. Then for the Oregonator model, in which Z is ferriin, we can write that

$$D_X \approx D_Y \ll D_Z \tag{14}$$

and

$$k_X \approx k_Y \ll k_Z \tag{15}$$

It is known[27,28] that with relationships 14 in the Oregonator model, Turing structures may arise from the spatially homogeneous unstirred stationary state. However, because of small values of D_X, D_Y, and D_Z in the AOT-BZ reaction, the size of these structures should be comeasurable with 1 μm, and hence, they may be hardly observable.

For single micelles, the value V_mN_A may vary from 20 to 1000 M^{-1}. If clusters are formed by 100−1000 micelles, the value V_cN_A may vary from 2×10^3 to $2 \times 10^5\ M^{-1}$. Hence, a probable variation range of V_cN_A lies between 10^3 and $10^6\ M^{-1}$.

A characteristic time of mixing, $t_{mix} = 1/k_{mix}$, for aqueous systems in small laboratory reactors ranges from 0.1 to 1 s at stirring rates from 200 to 1000 rpm. In viscous media, this time, naturally, becomes longer and may reach 1−10 s. The frequency-multiplying bifurcation in the AOT-BZ reaction was

TABLE 4: Ranges of the Main Parameter Values for AOT Microemulsion and the Corresponding Parameters for the PCA Model

range of parameters	k_{ex}, s^{-1}	V_cN_A, M^{-1}	k_{mix}, s^{-1}
for AOT microemulsion estimated by the experimental data	$10^{-2}-10^{3}$	$10^{3}-10^{6}$	$1-10$
for the PCA model studied in this work	$0.7-100$	$7 \times 10^{3}- 1 \times 10^{6}$	$k_{mix} = k_{ex}$
in which the bifurcation values $k_{ex} = k_{cr}$ are discovered	$1-6$	$(1100/k_{cr})^{1.76}$	$k_{mix} = k_{ex}$

discovered at high enough stirring.[14] Therefore in our computer experiment, we shall also use high stirring intensities at which the process of macromixing is limited by the mass exchange constant and the equality $k_{mix} \cong k_{ex}$ is fulfilled. The main characteristic constants of AOT microemulsion (k_{ex}, V_cN_A, and k_{mix}), determining the amplitude and frequency of concentration fluctuations, are summarized in Table 4.

The reaction rate constants of the elementary steps for the AOT-BZ reaction notably differ from those for the BZ reaction proceeding in the homogeneous aqueous media.[13] Thus, the constants in the Oregonator model may also differ from the accepted ones.[29] In this work, we use the basic set of the constants presented in Table 2. The concentration of A is a varying parameter ranging from [A] $\equiv a = 0.02$ M to $a = 1$ M. The interval $0.02-1$ M involves the Hopf bifurcation point for the model parameters used. With the given set of constants, the rate of Y particles' appearance in reaction R5 ($k_5b = 1\ s^{-1}$) is much larger than the rate of their disappearance in reaction R1 ($k_1a \ll k_5b$). Therefore the rate of a decrease and approach of [Y] to $[Y]_{cr} = ak_2/k_3$ is fully determined by the rate of reaction R1. Another peculiarity of the basic set of constants is the similarity of the kinetic curves [X] versus t and [Z] versus t.

4. Results and Discussion

To choose the parameter a we first obtained a bifurcation diagram by solving numerically the system of ordinary differential equations (ODE) for the Oregonator at various a. Typical shapes of kinetic curves obtained from the solution of the ODE for various a and the bifurcation diagram are presented in the Supporting Information in Figures 2S and 3S, respectively. It follows from the bifurcation diagram (Figure 3S) that at $a <$ 0.053 M, the system remains in the stationary state, while at $a >$ 0.054 M, the system exhibits sustained oscillations. The dependence of the oscillation period T_0 (obtained from the solution of the ODE) on a is presented in the Supporting Information in Figure 4S. An increase in a from 0.054 to 0.1 M is followed by a decrease in the minimum value $[X]_{min}$ of the oscillating value of [X] from 10^{-5} to 10^{-7} M and an increase in the period from 40 to 75 s. As a grows further, $[X]_{min}$ starts growing while the period T_0 starts shortening, in particular $T_0 = 41.7$ s at $a = 0.3$ M. Period T_0 passes through the maximum at the point $a = 0.1$ M. The data of Figures 2S−4S are used as the reference data for the results obtained by the PCA method.

The bifurcation diagram resulting from the solution of the stochastic Oregonator by the PCA method at high values of k_{ex} ($k_{ex} > 30\ s^{-1}$) completely matches the diagram obtained from the solution of the ODE. The dependence of the oscillation period T_∞ on a (shown in Figure 4S) also reproduces well the dependence of T_0 on a, though T_∞ is somewhat smaller than T_0 at all a. The symbol T_∞ denotes the maximum oscillation period T at $k_{ex} \rightarrow \infty$. For the basic set of the Oregonator model constants and at $V_cN_A > 10^5\ M^{-1}$, the period T ceases to depend on k_{ex} at $k_{ex} > 50\ s^{-1}$. With the growth in V_c, the difference between T_∞ and T_0 disappears. In view of the bifurcation diagram and the dependence of T_∞ on a, two values of the parameter a were chosen in the oscillation area for further studies by the PCA method: $a = 0.1$ M and $a = 0.3$ M.

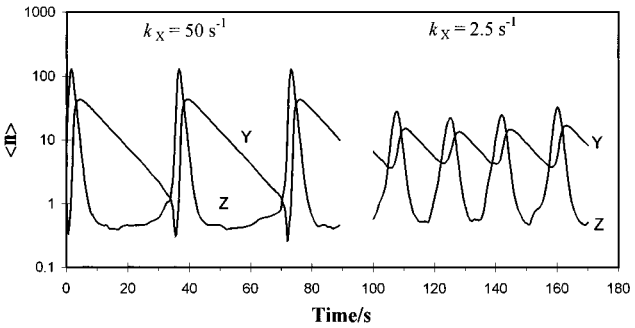

Figure 2. Kinetic curves for variables $\langle n_Y \rangle$ and $\langle n_Z \rangle$ obtained by the PCA method for the stochastic Oregonator model for various mass exchange constants k_X. A basic set of the Oregonator model constants was used at $a = 0.3$ M. PCA parameters: $N_0 = 32^2$, $V_cN_A = 4 \times 10^4\ M^{-1}$, $k_Z = 32\ s^{-1}$, $k_X = k_Y$, *StepDif* = 0.01 s, *StepMix* = 0.05 s, *Lev* = 3.

4.1. Evidence for Frequency-Multiplying Bifurcation. Kinetic Curves. Noticeable differences in the behavior of the stochastic and deterministic Oregonator emerge when the values of k_{ex} for X and Y become smaller, i.e., at a decrease in k_X and k_Y. Later, if not noted specifically, we shall use equal values of k_X and k_Y, and write only k_X meaning that $k_X = k_Y$. Characteristic kinetic curves for variables $\langle n_Y \rangle$ and $\langle n_Z \rangle$ at various k_X are shown in Figure 2. Variables $\langle n_X \rangle$, $\langle n_Y \rangle$, and $\langle n_Z \rangle$ determined in the PCA model by formula 10 relate to the variables [X], [Y], and [Z] as

$$\langle n_X \rangle = [X]V_cN_A, \quad \langle n_Y \rangle = [Y]V_cN_A, \quad \langle n_Z \rangle = [Z]V_cN_A \quad (16)$$

where V_c is the volume ascribed to a PCA cell. At high k_X ($k_X > 30\ s^{-1}$), the wave shape of oscillations obtained by the PCA method completely matches the wave shape of reference oscillations resulting from the ODE solution. At the same time, at low k_X ($k_X < 10\ s^{-1}$), the amplitude and oscillation period get smaller, and the shape of oscillations changes also, for instance, oscillations of the value $\langle n_Z \rangle$ assume the shape resembling sinusoidal oscillations (Figure 2). In addition, at small k_X, the relation abnormal for the oscillatory regime starts to hold:

$$\langle n_Y \rangle_{min} > \langle n_Y \rangle_{cr} \quad (17)$$

where $\langle n_Y \rangle_{cr} = [Y]_{cr}V_cN_A$ and $[Y]_{cr} = ak_3/k_2$ (critical concentration $[Y]_{cr}$ is determined from the equality of the rates of reactions R2 and R3). As is known, autocatalytic multiplication of X molecules in the Oregonator model, which is the necessary condition for oscillations, starts when $[Y] < [Y]_{cr}$. Relation 17 testifies to the presence of highly inhomogeneous states in the system of poorly coupled MOs.

To follow the origin of such extraordinary high-frequency oscillations, we determined the dependence of the oscillation period and amplitude on the mass exchange constant k_{ex}, on the cell volume V_c, and on the number of cells N_0 of the lattice. The ranges of the k_{ex} and V_cN_A values, characterized by the most considerable variations in the period T and oscillation amplitude, are given in Table 4. Notice that these ranges agree well with the analogous ranges estimated by the experimental data.

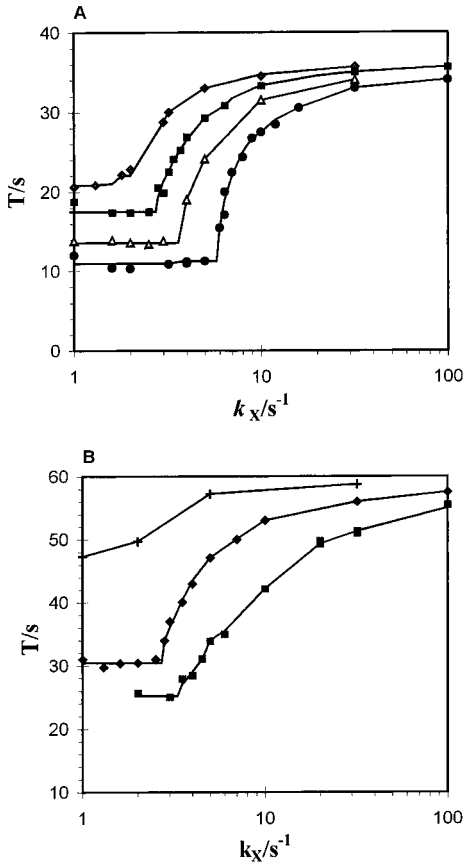

Figure 3. The dependencies of the oscillation period T on the mass exchange constant k_X in the stochastic Oregonator model at various volumes V_c of PCA cell. A basic set of the Oregonator model constants was used at (A) $a = 0.3$ M and (B) $a = 0.1$ M. PCA parameters: $N_0 = 32^2$, (+) $V_cN_A = 5 \times 10^5$ M^{-1}, (◆) $V_cN_A = 1 \times 10^5$ M^{-1}, (■) $V_cN_A = 4 \times 10^4$ M^{-1}, (△) $V_cN_A = 2 \times 10^4$ M^{-1}, (●) $V_cN_A = 1 \times 10^4$ M^{-1}, $k_Z = 32$ s^{-1}, $k_X = k_Y$, *StepDif* = 0.01 s for $k_X < 30$ s^{-1} and *StepDif* = 0.001 s for $k_X > 30$ s^{-1}, *StepMix* = 0.05 s, *Lev* = 3.

TABLE 5: Dependencies of the Periods T_∞ and T_m, the Ratio T_∞/T_m, and the Critical Constant of Mass Exchange Rate k_{cr} on the Molar Volume V_cN_A of a PCA Cell for the Stochastic Oregonator Model with the Basic Set of Constants at $a = 0.3$ M[a]

$V_cN_A \times$ M	$k_{cr} \times$ s	T_∞, s	T_m, s	T_∞/T_m
1×10^4	5.77	34	11.3	3
2×10^4	3.9	34.5	13.6	2.5
4×10^4	2.7	35	17.5	2
1×10^5	1.54	36	21	1.7

[a] PCA parameters: $N_0 = 32 \times 32$, $k_Z = 32$ s^{-1}, $k_X = k_Y$, *StepDif* = 0.01 s for $k_X < 30$ s^{-1} and *StepDif* = 0.001 s for $k_X > 30$ s^{-1}, *StepMix* = 0.05 s, and *Lev* = 3.

Dependencies of T on k_X at Various V_cN_A. The dependencies of the oscillation period T on k_X at various V_cN_A, shown in Figure 3, demonstrate the threshold changes in T with the variation in k_X in the vicinity of some critical point k_{cr}. Figure 3 shows that the oscillation period T decreases with a reduction in k_X, and as soon as k_X achieves a critical value k_{cr}, it ceases to change and attains its limiting minimum value T_m. Figure 3 also shows that the smaller the V_cN_A, the larger the decrease in the oscillation period. From the dependencies of the ratio T_∞/T_m on V_cN_A and of the critical value k_{cr} on V_cN_A presented in Table 5 for $a = 0.3$ M, one can see that the smaller the V_cN_A, the larger the T_∞/T_m and k_{cr}. Since with a decrease in the volume V_c of a cell the number of particles X, Y, and Z contained in it decreases and the fluctuation amplitude becomes larger, we may suggest that fluctuations play a decisive role in the effect observed. The comparison of parts A and B of Figure 3 also shows that the value of a has hardly any effect on the dependencies $T(k_X)$.

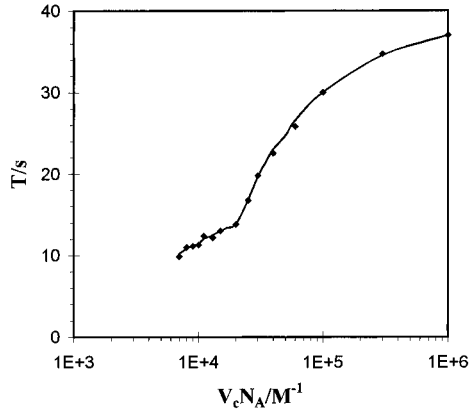

Figure 4. The dependencies of the oscillation period T on V_cN_A. Parameters: $a = 0.3$ M $k_X = k_Y = 3.2$ s^{-1}; the remaining parameters are the same as in Figure 3.

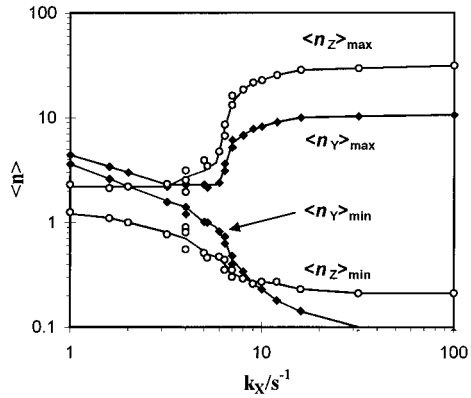

Figure 5. The dependencies of the maximum and minimum values of $\langle n_Z \rangle$ and $\langle n_Y \rangle$ on k_X in the stochastic Oregonator model at $a = 0.3$ M and $V_cN_A = 1 \times 10^4$ M^{-1}; the remaining parameters are the same as in Figure 3.

The difference $T - T_m$, which can be defined as the order parameter, depends on k_X near the critical point k_{cr} at $k_X > k_{cr}$ as

$$(T - T_m) \propto (k_X - k_{cr})^\beta \qquad (18)$$

where $\beta = 1/2$. Such a dependence of the system order parameter on the controlling parameter $(k_X - k_{cr})$ with the critical index $\beta = 1/2$ is typical for the equilibrium phase transition of the second order and for nonequilibrium phase transitions.[30,31] The dependencies of $(T - T_m)$ on $(k_X - k_{cr})^{1/2}$ at different a and V_cN_A are given in the Supporting Information in Figure 5S.

Dependence of T on V_cN_A at k_X = Constant. As follows from Figure 3, at a value of k_X such that $2 < k_X < 5.7$, the threshold dependencies of the period T on V_c, analogous to the dependencies of T on k_X, may be obtained. Such an example is shown in Figure 4. One can also see from Figure 4 that the period T tends to some limit at $V_cN_A \rightarrow \infty$. It is evident that this limit is the period $T_0 = 41.7$ s of the deterministic Oregonator.

Dependence of Oscillation Amplitude on k_X. Similar to the period T, the oscillation amplitude undergoes drastic change at the critical point. Figure 5 shows the dependencies of the minimum and maximum values of $\langle n_Y \rangle$ and $\langle n_Z \rangle$ on k_X. The analogous dependencies for the other values of a and V_cN_A are presented in the Supporting Information in Figures 6S and 7S.

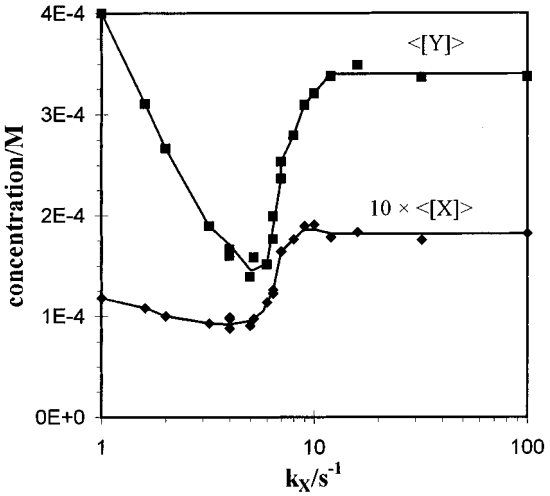

Figure 6. The dependencies of the ⟨[Y]⟩ and 10⟨[X]⟩ averaged over the oscillation period on k_X for the stochastic Oregonator. All the parameters are the same as in Figure 5.

As follows from Figure 5, a sharp decrease in the oscillation amplitude ($\langle n_Y\rangle_{max} - \langle n_Y\rangle_{min}$ and $\langle n_Z\rangle_{max} - \langle n_Z\rangle_{min}$), beginning approximately at $k_X < 10\ s^{-1}$, stops at the critical point $k_{cr} = 5.7\ s^{-1}$, and at $k_X < k_{cr}$, the oscillation amplitude becomes more or less stable. For the case presented in Figure 5, the ratio of the oscillation amplitude at $k_X \le k_{cr}$ to that at $k_X \gg k_{cr}$ equals 10 and 5 for $\langle n_Z\rangle$ and $\langle n_Y\rangle$, respectively. The smaller the V_cN_A, the larger the extent of the amplitude fall and oscillation frequency growth with the k_X decrease. Figure 5 also shows that the abnormal inequality in eq 17 holds true at $k_X < 8\ s^{-1}$ because $\langle n_Y\rangle_{cr} = 0.3$ in this case. It is interesting to note that the dependence of amplitude on oscillation frequency has a linear character in the range $k_{cr} < k_X < 2k_{cr}$.

Dependence of the Substrate A Consumption Rate on k_X. Apart from the oscillation period and amplitude, in the range of $k_X \in (k_{cr}, 2k_{cr})$ drastic changes occur with the values of [Y] and [X] averaged over the oscillation period

$$\langle [Y]\rangle = \frac{1}{mT}\int_0^{mT} \frac{\langle n_Y\rangle}{V_cN_A}\,dt = \frac{\Delta t}{mT}\sum_{t=0}^{t=mT}\frac{\langle n_Y\rangle}{V_cN_A} \qquad (19)$$

$$\langle [X]\rangle = \frac{1}{mT}\int_0^{mT} \frac{\langle n_X\rangle}{V_cN_A}\,dt = \frac{\Delta t}{mT}\sum_{t=0}^{t=mT}\frac{\langle n_X\rangle}{V_cN_A} \qquad (20)$$

where Δt is the constant time interval through which the values of all the system variables are written in the file ($T \gg \Delta t \gg \tau$) and m is the number of the whole periods. The values ⟨[Y]⟩ and ⟨[X]⟩ determine the substrate A consumption rate in reactions R1 and R3, averaged over the period. Substrates A and B serve as the source of energy, which supports oscillations. Since with the chosen constants of the Oregonator model the substrate B consumption rate, $v_5 = bk_5[Z]$, is 2 times larger than the substrate A consumption rate in reaction R3, $v_5 = 2v_3$, the dependence of ⟨[Z]⟩ on k_X adds no new information to that supplied by the dependence of ⟨[X]⟩ on k_X.

Figure 6 presents the dependencies ⟨[Y]⟩ and ⟨[X]⟩ on k_X. As follows from Figure 6, the values ⟨[Y]⟩ and ⟨[X]⟩ reach stationary level at $k_X > 2k_{cr}$ ($2k_{cr} = 11.4\ s^{-1}$), while at $k_{cr} < k_X < 2k_{cr}$, the values ⟨[Y]⟩ and ⟨[X]⟩ change drastically (by approximately 2 times) which means a change in the energy consumption (substrates A and B) by the system of slightly coupled stochastic oscillators. It is interesting to note that at $k_X > 2k_{cr}$, when the values ⟨[Y]⟩ and ⟨[X]⟩ cease to change, the period T continues growing and achieves its limiting value T_∞ only at $k_X \gg 2k_{cr}$. At $k_X < k_{cr}$, the values ⟨[Y]⟩ and ⟨[X]⟩ resume their growth, which is caused by the large mass exchange constant $k_Z = 32\ s^{-1}$. For the case of $k_Z = k_X = k_Y = k_{ex}$ that will be discussed later, the values ⟨[Y]⟩ and ⟨[X]⟩ do not grow at $k_{ex} < k_{cr}$. The considered peculiarities of the dependencies of ⟨[Y]⟩ and ⟨[X]⟩ on k_X hold in the entire studied range of the V_cN_A values from 10^4 to $10^5\ M^{-1}$. The dependencies of ⟨[Y]⟩ and ⟨[X]⟩ on k_X for various a and V_cN_A are given in the Supporting Information in Figures 8S and 9S.

TABLE 6: Possible Sequences of the Stochastic Oregonator Reactions Leading to the Dead-End Combinations of Numbers n_X, n_Y, and n_Z in an Isolated PCA Cell

reaction	n_X	n_Y	n_Z	reaction	n_X	n_Y	n_Z
R5′	0	1	2	R5′	0	1	3
R1	0	2	0	R1	0	2	1
R2	1	1	0	R2	1	1	1
	0	0	0		0	0	1

Dependence of T on N_0. The experiments on how the oscillation period depends on the total number N_0 of the elementary cells demand special care. The matter is that in the Oregonator model (reactions R1−R4 + R5′), where the variables n_X, n_Y, and n_Z are represented by whole numbers, there are the dead-end combinations of these numbers at which the chemical reactions, proceeding in a cell, stop. Table 6 presents some possible sequences of the reactions which lead to the dead-end combinations (0, 0, 1) and (0, 0, 0), where the numbers in the brackets equal n_X, n_Y, and n_Z, respectively. The variations given in Table 6 are highly probable for small-volume cells with few particles. If both the amount of cells N_0 and cell volume V_c are small, the contribution of the cells with the dead-end combinations to the dynamics of the entire system grows, which shows itself in the extension of the chemical processes, and, consequently, in the longer oscillation period. The only way for a cell to leave a dead-end state is to perform mass exchange with the adjacent cells. If we enlarge the mass exchange constant k_{ex} up to values of the order of $(\tau^{-1})_{max}$, where τ is determined by formula 11, then the influence of the cells in the dead-end states will be nullified even for small N_0.

With the account of the peculiarities mentioned above which proved to be significant only for $N_0 < 10^2$, we found that the oscillation period is independent of the amount of cells N_0 for $V_cN_A = 4 \times 10^4\ M^{-1}$ if $N_0 > 16^2$ and for $V_cN_A = 1 \times 10^4\ M^{-1}$ if $N_0 > 32^2$; i.e., the period is independent of product N_0V_c if N_0V_c is large enough, $N_0V_cN_A > 10^7\ M^{-1}$. This relates both to the period T_∞ and the period T_m. In these experiments, the value N_0 was enlarged up to 128^2. As N_0 was taken larger, the stirring level *Lev* increased consequently too,[20] and the equality $k_{mix} = k_{ex}$ was held.

The independence of T_m from N_0 at rather high N_0V_c allows us to say that the observed effect of oscillation frequency multiplication with a decrease in the coupling strength between MOs is not a result of mere summing up of oscillations produced by few (10−100) stochastic oscillators with noncorrelated phases. To the contrary, we may state that the emergence of high-frequency oscillations with the period T_m results from weak synchronization of stochastic MOs.

Kinetic Curves of Dispersions. The dependencies of the dispersions σ_X^2, σ_Y^2, and σ_Z^2 on time justify the last statement. At $k_X \gg k_{cr}$, for any phase of oscillations, the following relationships hold true: $\sigma_X^2 \cong \langle n_X\rangle$, $\sigma_Y^2 \cong \langle n_Y\rangle$, and $\sigma_Z^2 \cong \langle n_Z\rangle$. This testifies to the equilibrium Poisson distribution of X, Y, and Z particles among the cells and, hence, to the complete synchronization of MOs. At $k_X \le k_{cr}$ only the relation $\sigma_Z^2 \cong \langle n_Z\rangle$ holds, while the dispersions σ_X^2 and σ_Y^2 start to depend

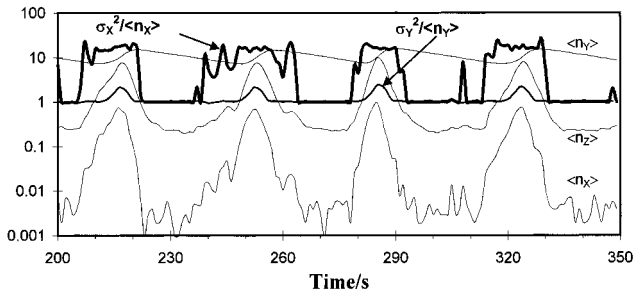

Figure 7. The dependencies of the dispersions σ_X^2 and σ_Y^2 (as ratios $\sigma_X^2/\langle n_X\rangle$ and $\sigma_Y^2/\langle n_Y\rangle$) on time for the stochastic Oregonator at $a = 0.3$ M and $k_1 = 0.05$ $M^{-1}s^{-1}$; the remaining Oregonator parameters are the same as in the basic set of constants. PCA parameters: $N_0 = 32^2$, $V_cN_A = 4 \times 10^4$ M^{-1}, $k_Z = 30$ s^{-1}, $k_X = k_Y = 1.6$ s^{-1}, *StepDif* = 0.01 s, *StepMix* = 0.05 s, *Lev* = 3. To mark the oscillation phase, the dependencies of $\langle n_X\rangle$, $\langle n_Y\rangle$, and $\langle n_Z\rangle$ on time are also given by thin lines.

on the oscillation phase as is shown in Figure 7. The largest difference between either $\sigma_X^2/\langle n_X\rangle$ or $\sigma_Y^2/\langle n_Y\rangle$ and unity is observed in the fast phase of the autocatalytic growth of X molecules ($k_3a = 6$ s^{-1}) and in the following fast phase of Z-to-X conversion ($k_5b = 1$ s^{-1}). During the slow phase of the Y-to-X conversion (reaction R1, $k_1a = 0.015$ s^{-1}), the distribution of all the particles among the cells becomes Poissonian, and hence, MOs at this time interval are synchronized.

4.2. Scenario of the Emergence of Frequency-Multiplying Bifurcation. As Figure 7 shows, the dispersion σ_X^2 is the first of σ_X^2 and σ_Y^2 to deviate from the equilibrium value. On this basis, we may suggest the following scenario for the oscillation frequency multiplication. Let all the MOs be synchronized, and let $\langle n_Y\rangle \gg \langle n_Y\rangle_{cr}$ (a slow phase of reaction R1) at the initial moment of time. Then, as a result of the probability character of the reactions in MV (reaction R1, in particular) and of the equilibrium fluctuations in the number of Y particles (n_Y) due to the mass exchange between the neighboring MVs, the number n_Y lowers randomly below the critical value $\langle n_Y\rangle_{cr}$ in few cells (or even in one cell). In these cells, the autocatalytic multiplication of X particles may start. If mass exchange constants k_X and k_Y are large, the critical fluctuation, $n_Y < \langle n_Y\rangle_{cr}$, disappears, while in the opposite case, when these constants are small enough, autocatalysis starts to develop in the cells with critical fluctuations (nuclei) and then spreads to the other cells which take part in mass exchange with the nuclei. Z Particles quickly forming in these cells (in the cause of reaction R3) and Y particles resulting from them (in the cause of reaction R5′) do not allow the average value $\langle n_Y\rangle$ become lower than $\langle n_Y\rangle_{cr}$. At this time interval (phase of reactions R3 and R5), the values $\sigma_X^2/\langle n_X\rangle$ and $\sigma_Y^2/\langle n_Y\rangle$ differ notably from unity. This mechanism explains why the oscillation period T shortens when k_X and k_Y ($k_X = k_Y$) decrease, but tells nothing about why the high-frequency oscillations occur with more or less regular period T_m if autocatalysis starts accidentally in an arbitrary cell.

In the cause of further analysis, we followed the behavior of an individual separate stochastic oscillator and the variation in the oscillation period in response to a decrease in the lattice size up to $N \times N = 2 \times 2$ at extremely high values of k_{ex} ($k_X = k_Y = k_Z = k_{ex}$), above which the oscillation period is no longer sensitive to k_{ex}. As mentioned above, for small-size lattices, this requirement is satisfied with the proviso that $k_{ex} \geq (1/\tau)_{max}$. Figure 8 shows the $\langle n_Z\rangle$ oscillation pattern for $N \times N = 2 \times 2$ at $k_{ex} = 1000$ s^{-1}. With such a high k_{ex}, a 2×2 cell lattice may be considered as a single stochastic oscillator because the intercellular mass exchange rate is much higher than the rate of chemical reactions. As may be seen in Figure 8, the oscillations of individual MO are of stochastic type: a period

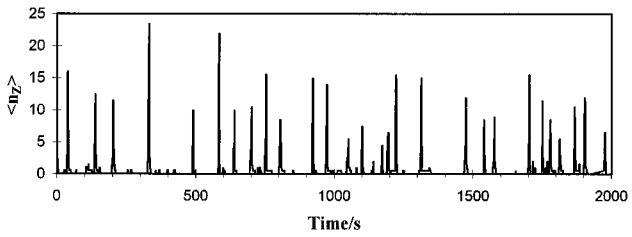

Figure 8. Kinetic curve for $\langle n_Z\rangle$ obtained by the PCA method for the stochastic Oregonator with the basic set of constants at $a = 0.1$ M and $V_cN_A = 4 \times 10^4$ M^{-1}. PCA parameters: $N_0 = 2^2$, $k_X = k_Y = k_Z = k_{ex} = 1000$ s^{-1}.

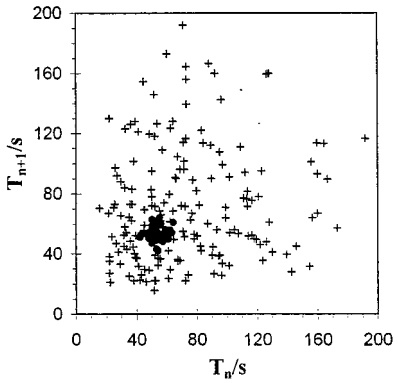

Figure 9. The dependence of the subsequent period T_{n+1} on the previous period T_n (next-period map) for the oscillations (+) presented in Figure 8 and for oscillations with the same Oregonator parameters (●) simulated on the lattice with the following parameters: $N_0 = 16^2$, $k_X = k_Y = k_Z = k_{ex} = 160$ s^{-1}, *StepMix* = 0.05 s, *Lev* = 3, $V_cN_A = 4 \times 10^4$ M^{-1}.

and amplitude vary randomly. But as soon as the amount of cells in a lattice increases, the oscillations acquire regular character. Figure 9 presents the dependence of the subsequent period T_{n+1} on the previous period T_n for the oscillations shown in Figure 8 and for the same model of oscillations but simulated on a 16×16 cell lattice, where T_n is the duration of the n-th period of oscillations. Figure 10S in the Supporting Information shows the analogous dependencies of T_{n+1} on T_n for a larger value of V_c ($V_cN_A = 5 \times 10^5$ M^{-1}).

As follows from Figure 9 (and Figure 10), with a larger size of the lattice, the dispersion of the periods T_n and, hence, the stochastisity of oscillations decrease markedly, while the averaged value of the periods, $\langle T_n\rangle$, varies slightly. The dependencies of T_{n+1} on T_n obtained for $N \times N = 2 \times 2$ at various V_cN_A show that the smaller the V_c, the larger the dispersion in T_n under otherwise identical conditions. It may also be noticed that the minimum value of the period T_n differs only slightly from the limiting value of the period T_m at equal V_cN_A. For instance, it may be seen from Figure 9 that $(T_n)_{min} = 20-25$ s, while it follows from Figure 3B that $T_m = 24-25$ s at the same $V_cN_A = 4 \times 10^4$ M^{-1}. On the basis of the proximity of the corresponding values of $(T_n)_{min}$ and T_m

$$(T_n)_{min} \cong T_m \tag{21}$$

we may assume that the oscillation frequency multiplication originates from the stochastisity of individual microoscillators. If autocatalytic multiplication of X particles starts in any of the numerous MOs, this "triggers" all the rest MOs, though the value of n_Y in all these cells−MOs has not yet become as low as the critical $\langle n_Y\rangle_{cr}$.

To substantiate the above assumption, we obtained the distribution of a large number (more than 1000) of periods of oscillations over the values of T_n (histogram) for the stochastic

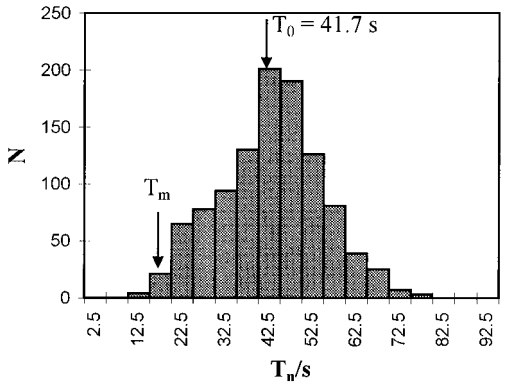

Figure 10. Histogram for an ensemble of 1100 periods T_n obtained for the stochastic Oregonator with the basic set of constants at $a = 0.3$ M and $V_cN_A = 4 \times 10^4$ M^{-1}; $N_0 = 2^2$, $k_X = k_Y = k_Z = k_{ex} = 2500$ s^{-1}. Along the abscissa axis, the middle values of the 5-s-intervals are plotted (the summation of the number of periods were done over 5-s-intervals).

Oregonator simulated on a 2×2 cell lattice at the extremely high mass exchange constants. The results for the case of $V_cN_A = 4 \times 10^4$ M^{-1} and $a = 0.3$ M are presented in Figure 10. The histogram maximum falls exactly on the oscillation period $T =$ 41.7 s of the deterministic Oregonator (the value $T = 41.7$ s was obtained from the numeric solution of the ODE for the Oregonator model with the corresponding parameters) and agrees well with the averaged value of $\langle T_n \rangle = 42.9$ s. The minimum values of T_n closely agree with the value of $T_m =$ 17.5 s for $k_{ex} \leq k_{cr}$ when large lattices are used (see Figure 3A). The histogram (Figure 10) also shows that there are the periods with $T_n < T_m$. A more thorough analysis, however, indicates that the emergence of these periods relates to the extremely low values of oscillation amplitudes (small peaklets) which only slightly exceed the background level (level of noise). These small peaklets are probably unable to stimulate autocatalysis in the whole system when a large number of cells are involved.

All the data presented in Figures 2−10 allow us to characterize the discovered effect as the bifurcation of oscillation frequency multiplication in the system of a large number of diffusionally coupled stochastic MOs at their intense stirring and to state that this bifurcation is caused by internal fluctuations of the system.

4.3. Connection between the Frequency-Multiplying Bifurcation and the Main Kinetic Constants, i.e., k_X, k_Y, k_Z, k_{mix}, and γ_i. Connection between the Bifurcation and k_X. So far we changed the values of $k_X = k_Y$ at $k_Z =$ constant. Thus, we are unable to conclude which one of the mass exchange constants, k_X or k_Y, leads to the bifurcation of frequency multiplication. To solve this problem, we conducted computer experiments considering the following cases: (i) $k_Y = k_Z =$ constant, k_X is variable and (ii) $k_X = k_Z =$ constant, k_Y is variable. It turned out that in the cases when the constant k_X remained unchanged, the variations in the period T were slight, and vice versa, when the constant k_X was a variable, the variations in the period T were pronounced. Table 7 presents some results that justify that the observed bifurcation mainly depends on k_X.

The Case of $k_X = k_Y = k_Z$. We may conclude as well that for such an important case as $k_X = k_Y = k_Z = k_{ex}$ the oscillation frequency multiplication may also be observed when k_{ex} decreases. The results of the computer experiments for this case are presented by curve 3 in Figure 11. Curve 2 in Figure 11 is the reference curve with the same model parameters as in the aforementioned case when $k_X = k_Y$ are variables and k_Z is constant. Unlike Figure 3, in Figure 11 along the abscissa axis,

TABLE 7: Dependence of T on k_X, k_Y, and k_Z[a]

k_X, s^{-1}	k_Y, s^{-1}	k_Z, s^{-1}	T, s
1.6	1.6	32	17.4 ± 0.8
1.6	1.6	1.6	16.7 ± 0.8
1.6	5	1.6	18.8 ± 0.7
5	1.6	1.6	28.8 ± 0.3
5	5	5	30.1 ± 0.3
5	5	32	29.3 ± 0.9

[a] A basic set of the Oregonator constants was used at $a = 0.3$ M. PCA parameters: $N_0 = 32 \times 32$, $V_cN_A = 4 \times 10^4$ M^{-1}, *StepDif* = 0.01 s, *StepMix* = 0.05 s, *Lev* = 3.

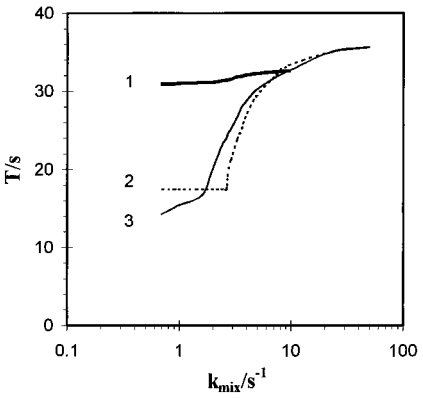

Figure 11. The dependencies of the oscillation period T on the macromixing constant k_{mix} for the stochastic Oregonator with the basic set of constants and $a = 0.3$ M. PCA parameters: *Lev* = 3, $V_cN_A = 4 \times 10^4$ M^{-1}, the value of *StepMix* is the variable for curve 1, $k_Z = k_X = k_Y = k_{ex} = 10$ s^{-1}. For curves 2 and 3, *StepMix* = 0.05 s; for curve 2, $k_Z = 32$ s^{-1}, $k_X = k_Y = k_{ex} = k_{mix}$; for curve 3, $k_X = k_Y = k_Z = k_{ex} = k_{mix}$.

the constant k_{mix} is plotted, which equals $k_X = k_Y = k_{ex}$ (see Figure 1) for the parameters of the PCA at which curves 2 and 3 are obtained. According to Figure 11, for $k_X = k_Y = k_Z = k_{ex}$, the oscillation period T also shortens when k_{ex} decreases. At some critical point k_{cr} ($k_{cr} \cong 1.7$ s^{-1}), the rate of changes in T, dT/dk_{ex}, decreases abruptly but does not reach zero, as in the case of curve 2. The dependencies of maximum and minimum values of $\langle n_Y \rangle$ and $\langle n_Z \rangle$ on k_{ex} and the dependencies of $[\langle Y \rangle]$ and $[\langle X \rangle]$ on k_{ex} are analogous to the dependencies presented in Figures 5 and 6 and are given in the Supporting Information in Figures 11S and 12S.

Independence of the Bifurcation from Stirring Rate. Let us consider now curve 1 in Figure 11. As was shown in section 2, the rate of macromixing characterized by the constant k_{mix} depends on the mass exchange constant k_{ex} and on the convection intensity determined by values *StepMix* and *Lev*. All of the above computer experiments on the detection of the frequency-multiplying bifurcation were conducted at high stirring intensity, when the macromixing rate is limited by the micromixing rate and $k_{mix} = k_{ex}$. We checked the behavior of the system in the opposite case, when macromixing is limited by convection and $k_{mix} \ll k_{ex}$. In these experiments, the constant k_{mix} was diminished by means of a growth in the time step *StepMix* (see Figure 1B). The results of these experiments presented by curve 1 in Figure 11 show that the period T remains practically unchanged as k_{mix} decreases at $k_{ex} =$ constant. On the basis of the data from Figure 11, we may conclude that the bifurcation of oscillation frequency multiplication depends on the mass exchange constant k_{ex} and does not depend (or barely depends) on the stirring rate (at least for the basic set of the Oregonator constants).

Dependence of the Bifurcation on the Chemical Reaction Rate Constants. In conclusion let us consider briefly how some constants of the Oregonator model may affect the frequency-

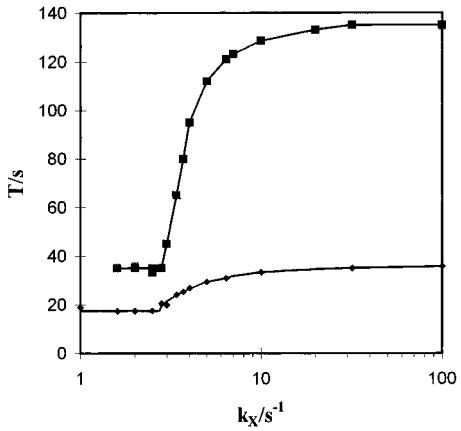

Figure 12. The dependencies of the oscillation period T on the mass exchange constant k_X in the stochastic Oregonator model at $a = 0.3$ M and various values of the constant k_1: (◆) $k_1 = 0.2$ M^{-1} s^{-1}, (■) $k_1 = 0.05$ M^{-1} s^{-1}. The remaining constants of the Oregonator are as in the basic set. PCA parameters: $N_0 = 32^2$, $V_cN_A = 4 \times 10^4$ M^{-1}, $k_Z = 32$ s^{-1}, $k_X = k_Y$, *StepDif* = 0.01 s for $k_X < 30$ s^{-1}, *StepDif* = 0.001 s for $k_X > 30$ s^{-1}, *StepMix* = 0.05 s, *Lev* = 3.

multiplying bifurcation. From the experiments and the theory on the stirring effects in the BZ reaction,[20,21] we know that the slower the inhibitor concentration approaches the critical point $[Y]_{cr}$, the more noticeable the fluctuations affect macrosystem dynamics. Since the bifurcation discovered in this work is of fluctuation nature, the ratio T_∞/T_m is expected to increase on condition that the rate of [Y] approach to $[Y]_{cr}$ slows down. This rate is controlled by the constant k_1. A decrease in k_1 does not change the position of the Hopf bifurcation point on the bifurcation diagram, but the oscillation period increases at the expense of R1 reaction slowing down, and the relaxation waveform of the oscillations becomes more pronounced (i.e., the ratio of time intervals at which [Z] grows rapidly and decreases slowly within a single period is increased). Figure 12 presents the dependencies of T on k_X for two different values of k_1. When k_1 decreases by a factor of 4 (from 0.2 M^{-1} s^{-1} to 0.05 $M^{-1}s^{-1}$), the ratio T_∞/T_m becomes nearly twice as much, growing from 2 to 3.8, while the critical constant k_{cr} ($k_{cr} \cong 2.8$ s^{-1}) remains unchanged.

5. Conclusion

With the theoretical method of the PCA, the bifurcation of oscillation frequency multiplication has been found at a decrease in the constant of mass exchange (or coupling strength) between a large number of identical stochastic microoscillators−Oregonators under their turbulent stirring. Either with a decrease in the coupling strength between MOs or with the reduction of the spatial size of MV−MO, the oscillation frequency of the entire system of coupled MOs starts to grow, and at some critical point, the rate of this growth changes in a threshold manner as in the nonequilibrium phase transitions or in the equilibrium phase transitions of the second order. At high mass exchange constants and at rather large sizes of the whole system, when the product N_0V_c is large, the oscillation frequency of the system of coupled stochastic MOs coincides with the oscillation frequency of the deterministic macrooscillator.

A mechanism for the oscillation frequency multiplication related to the stochastisity of a MO has been suggested. Frequency multiplication occurs when the coupling strength between MOs is neither too large nor too small. When the mass exchange constant k_{ex} is large, so that $k_{ex} > \gamma_i$, where γ_i are the rate constants for reactions R1−R5 presented in Table 2, then the "individuality" (or "stochastisity") of microoscillators is dampened and they oscillate in-phase with the most probable frequency $\cong T_0^{-1}$. At too low of a rate of mass exchange, when $k_{ex} < \gamma_i$, the coupling between MOs disappears and chaos follows; no oscillations of the entire system are observed in this case. The entire coupled system exhibits the largest sensitivity to the coupling strength at the critical point k_{cr} where the mass exchange constant k_X has the same order of magnitude as the constant γ_3 ($\gamma_3 = k_3[A]$) of the activator exponential growth.

There exists a similarity between the experimentally observed[14] and theoretically found bifurcation of frequency multiplication. In experiment,[14] the spontaneous changes in the frequency of the initial oscillations in the AOT-BZ reaction increase with micellar radius decrease. A spontaneous increase in oscillation frequency may occur due to the structural transformations of microemulsion during the reaction or due to a change in the rates of chemical reactions when bromine is stored in the organic phase. In the experiments on stirring effects,[21] we showed that an increase in $[Br_2]$ results in a slower approach of $[Br^-]$ to the critical concentration $[Br^-]_{cr}$ and, hence, an increase in the relaxation wave form of oscillations. The latter, as we have shown, enlarges the changes in oscillation frequency as a result of the frequency-multiplying bifurcation. A real AOT-BZ reaction, naturally, is more complex than the system of coupled stochastic Oregonators and there may exist another reasons leading to spontaneous multiplication of oscillation frequency.

We have not considered yet such problems as (i) the effect of polydispersity and the fractal nature of the micellar clusters on the bifurcation of frequency multiplication, (ii) the behavior of the stochastic Oregonator at $V_cN_A \rightarrow 0$ and $N_0 \rightarrow \infty$, (iii) the behavior of the system at $k_{ex} \rightarrow 0$, and (iv) the simulation of more complex BZ reaction models and peculiarities of the AOT-BZ reaction.

Quite a separate class of problems emerges when the cells of the PCA lattice are not stirred. According to our preliminary results, either the stationary Turing structures (described in detail by Becker and Field[28]) or the synchronous oscillations of all coupled stochastic MOs may arise under the oscillatory regime of the Oregonator model in the unstirred distributed system. The transition from the synchronous oscillations to the stationary structures occurs as soon as the constants k_X and k_Y of mass exchange decrease. Thus, the PCA method applied to the stochastic distributed Oregonator makes it possible to study the competition between the Hopf bifurcation and Turing bifurcation in the presence of fluctuations. It is interesting to note that if one turns on the "stirring" procedure when the Turing structures are formed, the oscillations with the multiplied frequency $(T_m)^{-1}$ appear in the assembly of coupled stochastic Oregonators.

The effect of oscillation frequency multiplication observed in this work may probably be met not only in the assembly of stochastic Oregonators but also in any other large assembly of stochastic oscillators. In this case, analogous effects may emerge in such assemblies of excitable cells as brain neurons or heart cells because the activity of isolated excitable cells (for instance, neurons[18]) is similar to the operation of a stochastic oscillator.

Acknowledgment. I am grateful to L. S. Vanag for the critical reading of the manuscript. The research described in this publication was supported in part by the Russian Foundation for Basic Research through Grant 97-03-32436a.

Supporting Information Available: Figures 1S−12S mentioned in the text (13 pages). Ordering information is given on any current masthead page.

References and Notes

(1) *Oscillations and Traveling Waves in Chemical Systems*; Field, R. J., Burger, M., Eds.; Wiley: New York, 1985; Chapters 2−4.
(2) Balasubramanian, D; Rodley, G. A. *J. Phys. Chem.* **1988**, *92*, 5995.
(3) Eicke, H. F.; Kirta, P. In *Reverse micelles*; Luisi, P. L., Straub, B. E., Eds.; Plenum Press: New York, 1984; p 21.
(4) Lang, J.; Jada, A.; Malliaris, A. *J. Phys. Chem.* **1988**, *92*, 1946.
(5) Fletcher, P. D. I.; Howe, A. M.; Robinson B. H. *J. Chem. Soc., Faraday Trans. 1* **1987**, *83*, 985.
(6) Ray, S.; Bisal, S. R.; Moulik, S. P. *J. Chem. Soc., Faraday Trans. 1* **1993**, *89*, 3277.
(7) Huang, J. S.; Kim, M. W. *Phys. Rev. Lett.* **1982**, *47*, 1446.
(8) Eicke, H. F.; Borkivec, M.; Gupta, B. D. *J. Phys. Chem.* **1989**, *93*, 314.
(9) Maitra, A.; Mathew, C.; Varshney, M. *J. Phys. Chem.* **1990**, *94*, 5290.
(10) Almgren, M.; Jóhannsson, R. *J. Phys. Chem.* **1992**, *96*, 9512.
(11) Vanag, V. K.; Boulanov, D. V. *J. Phys. Chem.* **1994**, *98*, 1449
(12) Vanag, V. K.; Hanazaki, I. *J. Phys. Chem. A* **1997**, *101*, 2147.
(13) Vanag, V. K.; Hanazaki, I. *J. Phys. Chem.* **1996**, *100*, 10609.
(14) Vanag, V. K.; Hanazaki, I. *J. Phys. Chem.* **1995**, *99*, 6944.
(15) Jóhannsson, R.; Almgren, M.; Alsins, J. *J. Phys. Chem.* **1991**, *95*, 3819.
(16) (a) D'Aprano, A.; D'Arrigo, G.; Paparelli, A.; Goffredi, M.; Liveri, V. T. *J. Phys. Chem.* **1993**, *97*, 3614. (b) Koper, G. J. M.; Sager W. F. C.; Smeets, J.; Bedeaux, D. *J. Phys. Chem.* **1995**, *99*, 13291.
(17) Epstein, I. R.; Showalter, K. *J. Phys. Chem.* **1996**, *100*, 13132.
(18) Abarbanel, H. D. I.; Rabinovich, M. I.; Selverston, A.; Bazhenov, M. V.; Huerta, R.; Sushchik, M. M.; Rubchinskii, L. L. *Usp. Fiz. Nauk* **1996**, *166* (4), 363.
(19) Field, R. J.; Noyes, R. M. *J. Chem. Phys*. **1974**, *60*, 1877.
(20) Vanag, V. K. *J. Phys. Chem.* **1996**, *100*, 11336.
(21) Vanag, V. K.; Melikhov D. P. *J. Phys. Chem.* **1995**, *99*, 17372.
(22) Bendat, J. S.; Piersol, A. G. *Random Data Analysis and Measurement Procedures*; John Wiley & Sons: New York, 1986.
(23) Tachiya, M. In *Kinetics of Nonhomogeneous Processes*; Freeman, G. R., Ed.; 1987, Wiley: New York, p 575−650.
(24) Almgren, M. *Adv. Colloid Interface Sci*. **1992**, *41*, 9.
(25) Gehlen, M. H. *Chem. Phys. Lett.* **1993**, *212*, 362.
(26) Genkin, M. V.; Logunov, I. V.; Davydov, R. M.; Krylov, O. V. *Kinet. Katal.* (Rus) **1991**, *32*, 336.
(27) Rovinsky, A. B. *J. Phys. Chem.* **1987**, *91*, 4606.
(28) Becker, P. K.; Field, R. J. *J. Phys. Chem.* **1985**, *89*, 118.
(29) Mazzotti, M.; Morbidelli, M; Serravalle, G. *J. Phys. Chem.* **1995**, *99*, 4501.
(30) Horsthemke, W.; Lefever, R. *Noise-Induced Transitions*; Springer Series in Synergetics, Vol. 15; Haken, H., Ed.; Springer: Berlin, 1984.
(31) Nicolis, G.; Prigogine, I. *Self-Organization in Nonequilibrium Systems*; Wiley: New York, 1977.